First-principles calculations of carbon nanotubes adsorbed on diamond (100) surfaces

2008 J. Phys.: Condens. Matter 20 225016

(http://iopscience.iop.org/0953-8984/20/22/225016)

IOP PUBLISHING JOURNAL OF PHYSICS: CONDENSED MATTER

J. Phys.: Condens. Matter **20** (2008) 225016 (6pp) doi:10.1088/0953-8984/20/22/225016

First-principles calculations of carbon nanotubes adsorbed on diamond (100) surfaces

Li Yan[1], **Qiang Sun**[1] **and Yu Jia**[1,2,3]

[1] School of Physics and Engineering, Zhengzhou University, Zhengzhou 450001, People's Republic of China
[2] Materials Science and Technology Division, Oak Ridge National Laboratory, Oak Ridge, TN 37831-6062, USA

E-mail: jiayu@zzu.edu.cn

Received 15 February 2008, in final form 18 April 2008
Published 15 May 2008
Online at stacks.iop.org/JPhysCM/20/225016

Abstract

We report first-principles total-energy calculations on the adsorption of (3, 3) and (4, 4) single-walled carbon nanotubes (SWCNTs) on clean and hydrogenated diamond (100) surfaces. For the nanotubes adsorbed on the clean surface we find that the stable geometries for the nanotubes are on top of dimer rows and between two consecutive dimer rows where C–C chemical bonds between carbons of the nanotubes and the surface dimers are formed. The binding energies for a (3, 3) nanotube at the two sites are 2.26 and 0.83 eV Å^{-1}, while they are 1.74 and 0.36 eV Å^{-1} for a (4, 4) nanotube. Our results show that to reach the stable geometry the nanotubes initially experience weakly adsorbed states at the position ∼2.6 Å above the surface and then overcome a barrier of ∼0.7 eV. Concerning the electronic properties, the most noticeable feature is that for the most stable geometry the electronic structure of the adsorbed metallic nanotube becomes semiconducting, i.e. a small band gap appears, due to the formation of C–C bonds between the nanotube and the dimer atoms. As a result, the adsorbed metallic nanotubes are realized in a metal-to-semiconductor transition. In contrast, on the fully hydrogenated C(100) surface, the nanotubes are weakly adsorbed on the surface, preserving an almost unchanged metallic character.

(Some figures in this article are in colour only in the electronic version)

1. Introduction

Carbon nanotubes (CNTs) [1], consisting of graphite layers rolled up to seamless, nanometer-wide cylinders, have been a focus of research interest because of their unique electrical and mechanical properties as well as their potential applications for future nanoelectronic devices [2, 3]. It is well known that CNTs can be either metallic or semiconducting, depending on their chirality [4]. For example, the electronic character of all armchair CNTs with chiral indices (n, n) are metallic. Through physical or chemical modifications of the armchair CNT, its physical properties can be largely modified, especially its conductivity. The structural and electronic properties of CNTs modified by various substrates have been widely investigated by both experimental and theoretical studies [5–17]. Recent first-principles calculations have shown marvelous results of single-walled carbon nanotube (SWCNT) adsorption on both the clean and the hydrogenated Si(001) surfaces [5, 12–17]. Peng *et al* [5] demonstrated that metallic CNTs with small diameter can switch to a semiconductor or enhance its metallic character, depending on the contact properties between the CNTs and the surfaces at the different adsorption sites. Sque *et al* [6] extensively studied metallic CNTs with large diameter on the surface of diamond and no electronic band structure gap opening was found. The main challenge for the use of CNTs to build nanostructures and nanoelectronic devices is attachment to technologically important substrates. Lyding and collaborators [7–10] developed a method termed 'dry-contact' deposition to attach nanotube power to semiconductor

[3] Author to whom any correspondence should be addressed.

substrate and found simultaneous atomic resolution scanning tunneling microscopy (STM) images of isolated SWCNTs and the local H-passivated Si(100) substrate. Fascinating results have been attained by using the tip of an atomic force microscope in controlling CNT adsorption on silicon surfaces [18, 19]. Diamonds have been widely exploited in various technological applications [20–22] because of their unique mechanical, thermal, electronic and optical properties. In particular, diamond can be an appealing substitute of silicon in forming the basis of semiconductor devices. Though there are some papers which have described the interaction between the metallic CNT and semiconductor surfaces or between the semiconducting CNT and metal surfaces [23–27], a study of the interplay between metallic CNTs and diamond surfaces is still lacking [6].

The purpose of our present paper is to explore the interplay between the metallic CNT and the diamond surfaces. In the paper we present the results of extensive first-principles calculations of metallic (3, 3) and (4, 4) nanotubes adsorbed on both clean and hydrogenated diamond (100) surfaces. As is well known, both surfaces can be stable dimerized 2×1 structures [28–30]. The calculated C–C dimer bond length is 1.38 Å for the clean surface and 1.63 Å for the hydrogenated surface. They are in the expected range for typical double C–C bond lengths and single C–C ones. On such surfaces we consider four sites for the SWCNT adsorption and find that the stable geometries for the nanotubes are on top of the dimer rows and between two consecutive dimer rows where C–C chemical bonds between carbons of the nanotubes and the surface dimers are formed. For the most stable geometry, the electronic structure of the adsorbed metallic nanotube becomes semiconducting.

The rest of this paper is organized as follows. In section 2 we briefly describe the methods. In section 3 we present the calculated results for (3, 3) and (4, 4) nanotubes adsorbed on clean and hydrogenated diamond (100) surfaces and give some detailed discussions about the geometries and electronic structures of the nanotubes adsorbed at the different sites. Finally, conclusions are summarized in section 4.

2. Methodology

In our study, the first-principles calculations are performed by using the Vienna *ab initio* simulation package (VASP) [31, 32] within the framework of density functional theory (DFT) [33, 34]. We adopt ultrasoft pseudopotentials [35] to describe the interaction between core and valence electrons. Electron exchange and correlation effects are described by the generalized gradient approximation of Perdew *et al* [36, 37]. Kohn–Sham orbitals are expanded in a plane wave basis set with a cut-off energy of 300 eV. The K-space integration is made by summing over a Monkhorst–Pack mesh [38] within the surface Brillouin zone (SBZ). We use four k points in the surface Brillouin zone for a 6×1 surface unit cell. The Fermi level is smeared by the Gaussian method [39] with a smearing width of 0.1 eV. The diamond lattice constant is taken to be our calculated value of 3.568 Å, which is a little larger than the experimental value 3.567 Å. The diamond surface is simulated by periodic slabs and for a clean diamond surface, each slab contains ten C atomic layers and the bottom C layer is passivated by H atoms. For a hydrogenated diamond surface, the same atomic layers are used with the top-layer C atoms adsorbed by one layer of H atoms. The thickness of the vacuum region between the slabs is taken to be about 20 Å. Our supercell calculations are carried out using a 6×1 surface unit cell in describing the dimer reconstruction of the surface. The bottom C and saturated H atoms are fixed during structure optimization and the positions of the other atoms are relaxed until all force components are less than 0.05 eV Å^{-1}. Our unit cell contains 78–88 atoms for describing armchair (3, 3) and (4, 4) SWCNTs adsorbed on diamond (100) surface, respectively. The commensurability condition is applied by stretching the carbon nanotube by about 2.5% [6].

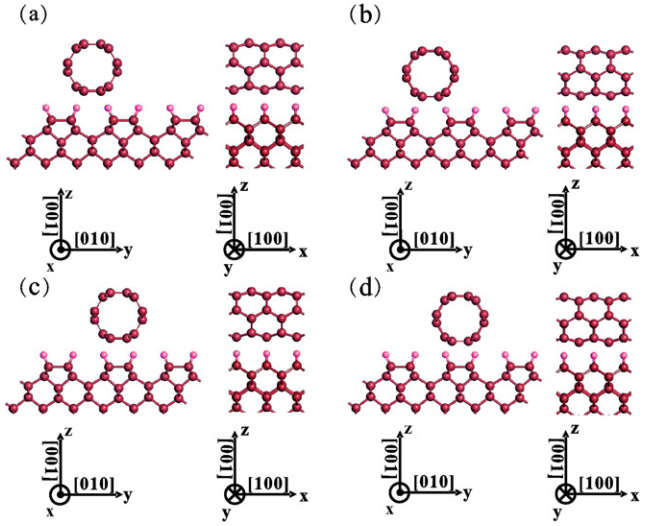

Figure 1. Four highly symmetrical adsorption sites of a (3, 3) SWCNT on a hydrogenated diamond (100) surface: (a) trench-top position; (b) trench-gap position; (c) dimer-top position; (d) dimer-gap position. Small (pink) spheres: hydrogens; large (dark red) spheres: carbons.

3. Calculations and results

For both the (3, 3) and (4, 4) SWCNTs on the clean and hydrogenated C(100) surfaces, four possible adsorption sites are considered: (i) the trench-top position; (ii) the trench-gap position; (iii) the dimer-top position; (iv) the dimer-gap position. The four adsorption geometries for a (3, 3) SWCNT adsorbed at the four sites on the hydrogenated C(100) surface are depicted in figure 1.

The adsorption energy E_{ads} is defined as

$$E_{\text{ads}} = (E_{\text{sub}} + E_{\text{cnt}} - E_{\text{sub+cnt}})/a,$$

where E_{sub}, E_{cnt} and $E_{\text{sub+cnt}}$ are the total energies of the diamond substrate, CNT and adsorbed system, respectively, and a is the dimension of the CNT along its axis in the surface unit cell.

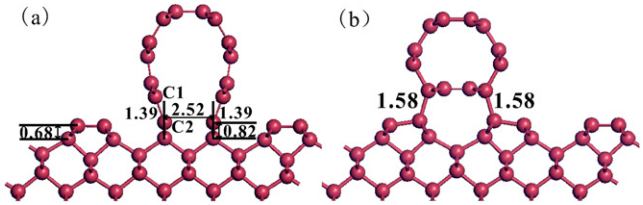

Figure 2. (a) Optimized atomic structure of a (3, 3) SWCNT adsorbed at the dimer-top position of the clean diamond (100) surface. (b) Optimized atomic structure of a (3, 3) SWCNT adsorbed at the trench-gap position of the clean diamond (100) surface. The distances between carbons are present in angstroms.

3.1. (3, 3) and (4, 4) SWCNTs adsorbed on the clean diamond (100) surface

Firstly, we study the SWCNTs adsorption on the clean C(100) surface. The calculated adsorption energies of the (3, 3) and (4, 4) SWCNTs at the four sites on the clean C(100) surface are presented in table 1. From the calculated results we see that the (3, 3) and (4, 4) SWCNTs adsorbed at the dimer-top position have the largest adsorption energies which are calculated to be 2.26 eV Å^{-1} and 1.74 eV Å^{-1}, respectively. They are chemisorbed at the position because of the formation of new chemical bonds between the SWCNTs and the surface. It is interesting to notice that in order to reach the chemisorbed states the nanotubes located at the dimer-top position beyond 2.6 Å above the surface should overcome a barrier of ∼0.7 eV. The optimized structure of the (3, 3) nanotube adsorbed at the dimer-top position is shown in figure 2(a). The chemisorbed (3, 3)/(4, 4) SWCNT at the dimer-top position forms two C–C bonds (per unit cell) with the surface dimer C atoms and the calculated C–C bond length is found to be 1.39 Å for the (3, 3) SWCNT and 1.40 Å for the (4, 4). The bond of the surface dimer is broken and the distance between the dimer C atoms has been elongated to be 2.52 Å. The optimized geometries of the chemisorbed SWCNTs show distortions compared to the isolated one and the diameters of the (3, 3) and (4, 4) SWCNTs are enlarged from 4.01 Å and 5.24 Å to 4.29 Å and 5.37 Å, respectively, and these distortions are obviously formed because of the formation of the CNT-surface chemical bonds.

The second stable adsorption site of the CNT is at the trench-top position. The calculated adsorption energies of the (3, 3) and (4, 4) SWCNTs are 0.83 eV Å^{-1} and 0.36 eV Å^{-1}, respectively. The calculated shortest C–C distances between the CNTs and the surface are 1.56 Å ((3, 3) CNT) and 1.57 Å ((4, 4) CNT). The bond properties between the CNTs and the surface should be weak chemical bonds.

At the dimer-gap and trench-gap positions, the SWCNTs are weakly adsorbed. The adsorption energies for the (3, 3) CNT at the two sites are 0.07 eV Å^{-1} and 0.14 eV Å^{-1}, while 0.03 eV Å^{-1} and 0.06 eV Å^{-1} for the (4, 4) CNT. We notice that at the trench-gap position the adsorption of the (3, 3) CNT is somewhat stronger (0.14 eV Å^{-1}), and figure 2(b) shows the optimized structure. For the equilibrium geometry, the shortest C–C distances between the CNT and the surface are found to be 1.58 Å. Though no chemical bonds between the CNT and the surface dimer are formed, the distortion of the CNT is dramatic: the lowest C atoms of the CNT move upwards severely and the surface C-dimers are buckled by 13 degrees. The calculated electronic structures for the adsorbed system given below show the metallic properties of the CNT adsorbed at the position enhanced.

Table 1. Adsorption energies (in eV) of (3, 3) and (4, 4) SWCNTs at the four adsorption sites on the clean C(100) surface.

CNT	Trench-top	Trench-gap	Dimer-top	Dimer-gap
(3, 3)	0.83	0.14	2.26	0.07
(4, 4)	0.36	0.06	1.74	0.03

Now we study the electronic structures of the SWCNTs adsorbed at the different sites on the surface. Figure 3(a) shows the electronic band structure of the (3, 3) SWCNT adsorbed on the dimer-top position. The most striking feature of the electronic band structure of the adsorbed system is the appearance of a band gap, which is similar to the result obtained by Peng *et al* [5] about a (3, 3) SWCNT adsorbed on Si(001). In the electronic band structure, J–Γ represents the direction parallel to the tube axis or dimer row, while Γ–J′ represents the direction perpendicular to the tube axis, i.e. along the surface normal. Along the Γ–J direction, there is no energy band across the Fermi level (E_F) and a gap of about 1.15 eV appears, indicating that the metallic (3, 3) SWCNT adsorbed at the dimer-top position converts to a semiconductor. The bands labeled by m_1, m_2, m_3 and m_4 are mixed CNT-surface states, while S_1, S_2, S_3 and S_4 could be assigned to diamond surface states. Figure 3(b) shows the projected density of states (PDOS) of the bonded carbon atoms (labeled as C1 and C2 in figure 2(a)) of the CNT and the surface dimer. By comparing the peaks of projected states (mainly projected P states) contributed by the carbon atoms from the CNT and the surface dimer, it can be found that there are four hybridization states, which are located at −1.60 eV, −1.00 eV, 0.75 eV and 1.25 eV, respectively. Because of the formation of the new bonds between the CNT and the surface, the hybridization and drastic changes in electronic structure of the adsorbed SWCNT compared to the isolated one should be expected. In order to further understand why the gap opens, we calculate the electronic structure of the deformed CNT, isolated by removing the diamond substrate, and figure 3(c) shows the calculated band structure of it. We learn in figure 3(c) that the deformed isolated CNT remains metallic in character. However, if we attach two H atoms to the deformed CNT at the two bottom carbon atoms to elucidate the effect of bonding on the electronic structure, it can be clearly found that by introducing the bonding the gap is reproduced in the band structure, as shown in figure 3(d). Hence it can be concluded that it is introducing the bonded atoms into the π electron network that makes the gap open, giving rise to an energy gap of 1.15 eV, which is also similar to the results obtained by Peng *et al* [5].

In figure 4, different charge density of the (3, 3) SWCNT adsorption on the dimer-top position is depicted as a contour plot to further elucidate the bond formation between the CNT and the substrate. The different charge density is defined by the

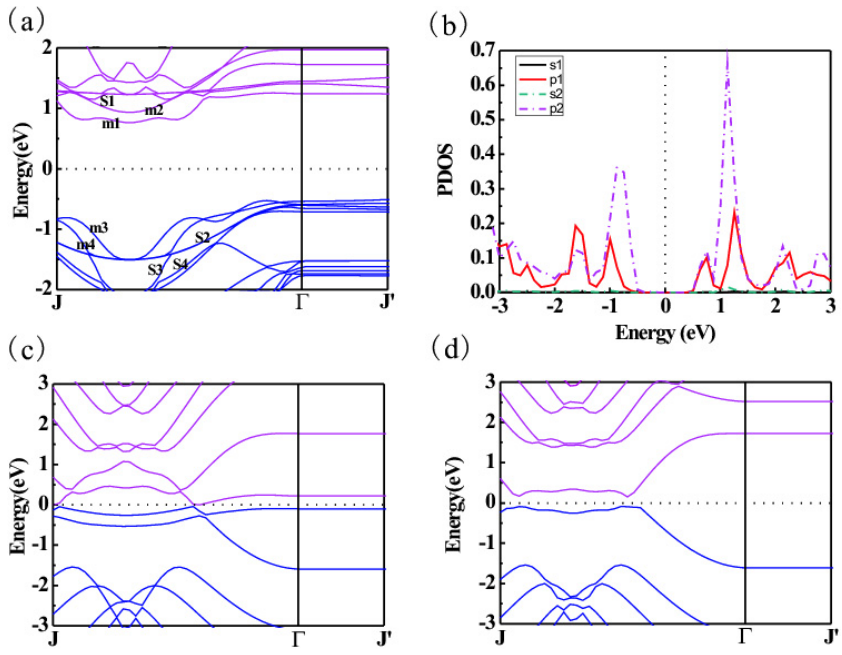

Figure 3. (a) Electronic band structure of the (3, 3) CNT adsorbed at the dimer-top position; (b) projected density of states of C1 and C2 of the adsorbed system; (c) electronic band structure of the optimized (3, 3) CNT isolated from the substrate; (d) electronic band structure of the isolated (3, 3) CNT with the bottom-most carbons saturated by hydrogen atoms. This explicitly introduces sp^3 bonded atoms into the π electron network and reproduces the band gap of 1.15 eV.

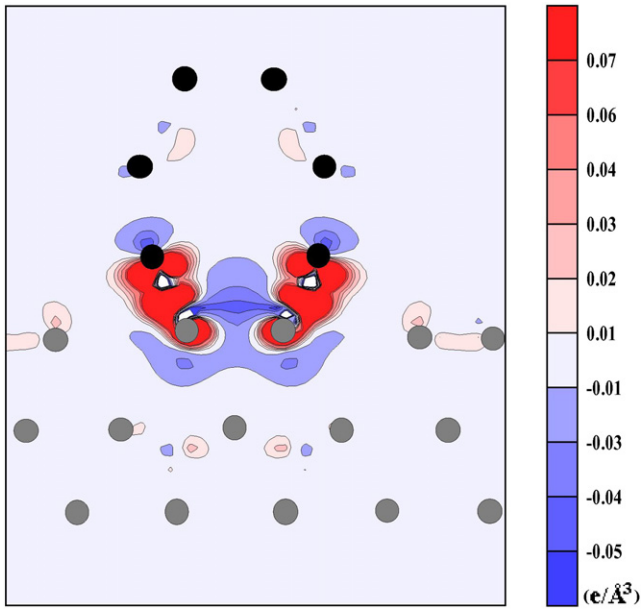

Figure 4. The different charge density contour plot for the (3, 3) CNT adsorption at the dimer-top position. The cutting plane is through the dimer and perpendicular to the surface. The carbon atoms of the CNT and the surface on the cutting plane are marked by black and gray spheres, respectively.

charge density difference between the adsorbed system and the isolated CNT plus the diamond surface, i.e. $\rho_{cnt+sub}-\rho_{cnt}-\rho_{sub}$, and the plane is through the surface dimer and perpendicular to the surface. The dramatic change upon the attachment of the CNT to the diamond substrate happens around the C1–C2

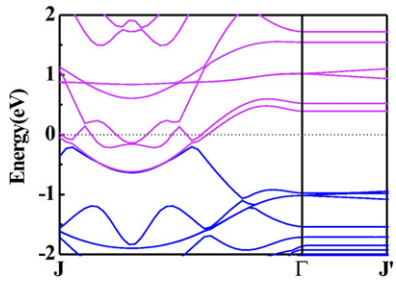

Figure 5. Electronic band structure of the (3, 3) CNT adsorption at the trench-gap position.

bonds formed between the CNT and the substrate. As a result of the hybridization between the C1 of the CNT and the C2 of the surface, charges are accumulated between the carbons C1 and C2, while they are decreased between the carbons of the surface dimer.

As mentioned above, the metallic character of the (3, 3) SWCNT is enhanced for the case of the SWCNT adsorbed at the trench-gap position (the optimized structure shown in figure 2(b)). The band structure of the adsorbed system is given in figure 5. As can be seen from the figure, the tube remains metallic in character. Since there are more bands across the Fermi level, the metallic character of the nanotube should be enhanced.

For the (4, 4) SWCNT adsorbed system, we also find that the adsorbed CNT at the dimer-top position realizes a metal-to-semiconductor transition, i.e. a band gap of about 1 eV opens in the electronic band structure. This value is a little smaller than the band gap of the (3, 3) CNT adsorbed at the same

Table 2. Adsorption energies (in eV) of (3, 3) and (4, 4) SWCNTs at the four adsorption sites on the hydrogenated C(100) surface.

CNT	Trench-top	Trench-gap	Dimer-top	Dimer-gap
(3, 3)	0.05	0.05	0.07	0.05
(4, 4)	0.01	0.01	0.01	0.01

position of the clean diamond (100) surface. It is interesting to notice that for the metallic CNT with smaller diameter a band gap opening could be seen as it chemisorbed on both Si [5] or C surfaces. However, for a metallic CNT with a larger diameter, for example, a (7, 7) CNT, this gap opening could not be found [6]. Therefore, it seems to infer that the bigger the chemisorbed metallic CNT diameter is, the smaller the obtained band gap is expected to become, until a critical diameter is reached, and then the metal-to-semiconducting transition no longer exists.

For the (4, 4) CNT adsorbed at the other positions, the electronic structures of the CNT still retain their metallic character due to the weak interaction between the (4, 4) CNT and the surface (see the adsorption energies of the (4, 4) CNT at the different positions in table 1).

3.2. (3, 3) and (4, 4) SWCNTs adsorbed on the hydrogenated diamond (100) surface

Now, we study the (3, 3) and (4, 4) SWCNTs adsorbed on the hydrogenated C(100) surface. Adsorption energies of the (3, 3) and (4, 4) CNTs at the four sites on the hydrogenated C(100) surface are shown in table 2. From the results of modeling (3, 3) SWCNT adsorption on the hydrogenated C(100) surface, we could learn that the adsorption of the SWCNT at the dimer-top position has the largest adsorption energy, which is about 0.07 eV $Å^{-1}$. The adsorption energies at the other sites are all about 0.05 eV $Å^{-1}$. It is reasonable to conclude that the adsorptions of the SWCNTs on the hydrogenated surface are physisorbed due to the low adsorption energies. All the nanotubes are located at about 2.23 Å above the surface.

When we consider the (4, 4) adsorption on the hydrogenated surface, it is found that the adsorption energies of the CNT at the four sites are ∼0.01 eV $Å^{-1}$, and the nanotube is located at about 2.35 Å above the surface.

Overall, given the low adsorption energies, the (3, 3) and (4, 4) nanotubes adsorbed on the hydrogenated diamond (100) surface are physisorbed. And the electronic structures of the nanotubes do not change much because of the weak interaction between the nanotubes and the surface. This finding is in agreement with the previous results about the SWCNTs adsorbed on the hydrogen-passivated Si substrates obtained by Miwa *et al* [16] and Albrecht and co-workers [13].

4. Conclusions

In summary, we have presented a comprehensive theoretical study of (3, 3) and (4, 4) armchair SWCNT adsorption on both the clean and hydrogenated diamond (100) surfaces. For the nanotubes adsorbed on the clean surface we find that the stable geometries for the nanotubes are on top of dimer rows (the dimer-top position) and between two consecutive dimer rows (the trench-top position) where C–C chemical bonds between carbons of the nanotubes and the surface dimers are formed. By selecting the adsorption of the CNTs at the dimer-top or the trench-gap position, the metallic character of the CNTs may change to semiconducting or be largely enhanced. However, on the hydrogenated diamond surface, the CNTs are physisorbed thanks to the low adsorption energies, and the electronic structures of the CNTs remain metallic in character.

Acknowledgments

We thank Professor Zhenyu Zhang at Oak Ridge National Laboratory and Professor Yuping Huo at Zhengzhou University for the helpful discussions. LY also thanks Mr Weiguang Chen and Dr S F Li for technical support. This work is supported by the NSF of China (No. 10574113) and partly by the Innovation Talents at the University of Henan Province, China.

References

[1] Iijima S 1991 *Nature* **354** 56
[2] Dresselhaus M S, Dresselhaus G and Eklund P C 1996 *Science of Fullerenes and Carbon Nanotubes* (San Diego, CA: Academic)
[3] Odom T W, Huang J L, Kim P and Lieber C M 2000 *J. Phys. Chem.* B **104** 2794
[4] Mintmire J W and White C T 1995 *Carbon* **33** 893
[5] Peng G W, Huan A C H, Liu L and Feng Y P 2006 *Phys. Rev.* B **74** 235416
[6] Sque S J, Jones R, Oberg S and Briddon P R 2007 *Phys. Rev.* B **75** 115328
[7] Albrecht P M and Lyding J W 2003 *Appl. Phys. Lett.* **83** 5029
[8] Ruppalt L B, Albrecht P M and Lyding J W 2004 *J. Vac. Sci. Technol.* B **22** 2005
[9] Albrecht P M and Lyding J W 2007 *Small* **3** 146
[10] Albrecht P M, Barraza-Lopez S and Lyding J W 2007 *Small* **3** 1402
[11] Kim Y-H, Leben M J and Zhang S B 2004 *Phys. Rev. Lett.* **92** 176102
[12] Barraza-Lopez S, Albrecht P M, Romero N A and Hess K 2006 *J. Appl. Phys.* **100** 124304
[13] Albrecht P M, Barraza-Lopez S and Lyding J W 2007 *Nanotechnology* **18** 095204
[14] Berber S and Oshiyama A 2006 *Phys. Rev. Lett.* **96** 105505
[15] Orellana W, Miwa R H and Fazzio A 2003 *Phys. Rev. Lett.* **91** 166802
[16] Miwa R H, Orellana W and Fazzio A 2005 *Appl. Phys. Lett.* **86** 213111
[17] Lee J-Y and Cho J-H 2006 *Appl. Phys. Lett.* **89** 023124
[18] Avouris Ph, Hertel T, Martel R, Schmidt T, Shea H R and Walkup R E 1999 *Appl. Surf. Sci.* **141** 201
[19] Hertel T, Martel R and Avouris Ph 1998 *J. Phys. Chem.* B **102** 910
[20] Amaratunga G A J 2002 *Science* **297** 1657
[21] Isberg J, Hammersberg J, Johansson E, WikstrÖm T, Twitchen D J, Whitehead A J, Coe S E and Scarsbrook G A 2002 *Science* **297** 1670
[22] Trew R J, Yan J-B and Mock P M 1991 *Proc. IEEE* **79** 598
[23] Okada S and Oshiyama A 2005 *Phys. Rev. Lett.* **95** 206804
[24] Tans S J, Verschueren A R M and Dekker C 1998 *Nature* **393** 49
[25] Martel R *et al* 1998 *Appl. Phys. Lett.* **73** 2447
[26] Nosho Y *et al* 2005 *Appl. Phys. Lett.* **86** 073105

[27] Nosho Y *et al* 2005 *Proc. 25th Spring Mtg of the Japan Society of Applied Physics (Saitama, Japan)* (Tokyo: Japan Society of Applied Physics) p 1684 (Extended Abstracts)
[28] Yang S H, Drabold D A and Adams J B 1993 *Phys. Rev.* B **48** 5261
[29] Zhang Z, Wensell M and Bernholc J 1995 *Phys. Rev.* B **51** 5291
[30] Furthmüller J, Hafner J and Kresse G 1996 *Phys. Rev.* B **53** 7334
[31] Kresse G and Furthmüller J 1996 *Phys. Rev.* B **54** 11169
[32] Kresse G and Hafner J 1993 *Phys. Rev.* B **47** 558
Kresse G and Hafner J 1994 *Phys. Rev.* B **49** 14251
[33] Hohenberg P and Kohn W 1964 *Phys. Rev.* **136** B864
[34] Kohn W and Sham L J 1965 *Phys. Rev.* **140** A1133
[35] Vanderbilt D 1990 *Phys. Rev.* B **41** 7892
[36] Perdew J P, Chevary J A, Vosko S H, Jackson K A, Pederson M R, Singh D J and Fiolhais C 1992 *Phys. Rev.* B **46** 6671
[37] Perdew J P, Burke K and Ernzerhof M 1996 *Phys. Rev. Lett.* **77** 3865
[38] Monkhorst H J and Pack J D 1976 *Phys. Rev.* B **13** 5188
[39] Methfessel M and Paxton A T 1989 *Phys. Rev.* B **40** 3616